Available online at www.sciencedirect.com
SCIENCE DIRECT
International Journal of Mass Spectrometry 246 (2005) 56–64
International Journal of Mass Spectrometry
www.elsevier.com/locate/ijms

Comparison of dissociation mechanism between collisionally activated dissociation and charge inversion using alkali metal targets for chlorophenol isomers

Shigeo Hayakawa [a,*], Yoshiaki Kawamura [a], Yutaka Takahashi [b]

[a] *Department of Chemistry, Graduate School of Science, Osaka Prefecture University, Gakuencho 1-1, Sakai, Osaka 599-8531, Japan*
[b] *MS R&D Group, Analytical Instrument Division, JEOL Ltd., 3-1-2 Musashino, Akishima, Tokyo 196-8551, Japan*

Received 4 June 2005; received in revised form 4 July 2005; accepted 5 July 2005
Available online 16 September 2005

Abstract

Chlorinated aromatic compounds are well-known environmental pollutants whose toxicities depend dramatically on the chlorine substitution pattern, making differentiation of chlorophenol isomers important for environmental analysis. Collisionally activated dissociation (CAD) spectra and charge inversion spectra of *ortho*-, *meta*-, and *para*-chlorophenols (ClC_6H_4OH) and their partially deuterated forms (ClC_6H_4OD) were measured using alkali metal targets. The peaks associated with $C_6H_4O^+$ and $C_5H_5Cl^+$ ions observed in the CAD spectra result from the loss of HCl and CO fragments, respectively, after the re-arrangement of the hydroxyl hydrogen atom. The peaks associated with $C_6H_4OH^-$ and $ClC_6H_4O^-$ ions observed in the charge inversion spectra result from Cl loss and from hydroxyl bond dissociation, respectively. Isomeric differentiation is possible based on the clear differences observed in the relative intensities of these pairs of peaks. Although the intensities of the peaks associated with $C_6H_4O^+$ relative to those of $C_5H_5Cl^+$ in the CAD spectra are independent of the target species, the intensities of the peaks associated with $C_6H_4OH^-$ relative to those of $ClC_6H_4O^-$ in the charge inversion spectra are target dependent. The isomeric dependence of the positive ion distribution patterns in the CAD spectra is proposed to be due to the differences in the rate of the hydrogen atom re-arrangement process. In contrast, the isomeric dependence of the negative ion distribution patterns in the charge inversion spectra is attributed to differences in the bond strength involved in the direct dissociation process in the neutral intermediate species.

Keywords: Charge inversion mass spectrometry; Dissociation mechanism; Isomeric differentiation; Chlorophenols; Alkali metal target

1. Introduction

Chlorinated aromatic compounds are well-known environmental pollutants, especially some isomers of poly-chlorinated dibenzo-*p*-dioxines (PCDDs) and poly-chlorinated dibenzofurans (PCDFs) which are extremely toxic to humans and animals [1–10], and their toxicity depends dramatically on the chlorine substitution pattern [1–3]. Since high-resolution gas chromatographic methods can separate structural isomers, and mass spectrometry is the most sensitive analytical method, the combination of high resolution gas chromatography and high resolution mass spectrometry (HRGC–HRMS) has been used widely for analysis of chlorinated aromatic compounds [11–17]. However, analysis of a single sample using capillary gas chromatography requires several minutes. In order to enable more rapid and sensitive analysis, various mass spectrometry/mass spectrometry (MS/MS) methods have been investigated [18–23]. Chlorophenols and dichlorobenzenes are constituent compounds of PCDDs and PCDFs, and so

Abbreviations: CAD, collisionally activated dissociation; PCDDs, poly-chlorinated dibenzo-*p*-dioxenes; PCDFs, poly-chlorinated dibenzofurans; MIKE, mass-selected ion kinetic energy; DEA, dissociative electron attachment; EI, electron ionization; ESA, electrostatic analyzer

* Corresponding author. Tel.: +81 72 254 9714; fax: +81 72 254 9931.
E-mail addresses: hayakawa@c.s.osakafu-u.ac.jp (S. Hayakawa), kawamura@mail.cias.osakafu-u.ac.jp (Y. Kawamura), tyutaka@jeol.co.jp (Y. Takahashi).

1387-3806/$ – see front matter © 2005 Elsevier B.V. All rights reserved.
doi:10.1016/j.ijms.2005.07.001

the discrimination of isomeric chlorophenols (ClC_6H_4OH) and dichlorobenzenes ($C_6H_4Cl_2$) by MS/MS methods is indispensable for high throughput analysis of environmental pollutants.

One of the authors has already reported clear discrimination of dichlorobenzene isomers [24] and the hydrocarbon isomers $C_2H_2^+$ and $C_3H_4^+$ [25–28] using charge inversion mass spectrometry. It was demonstrated that this discrimination is possible due to the dissociation of energy selected neutrals formed by near-resonant neutralization with alkali metal targets [29–32]. Neutralization–reionization mass spectrometry (NRMS) that used alkali metal target had also provided the discrimination of isomers [33–37]. In the present work, the discrimination of chlorophenol isomers using the charge inversion mass spectrometry was investigated.

Only the *ortho*-isomer of the chlorophenols was distinguished from the *meta*- and *para*-isomers by standard electron ionization (EI) spectra [38]. Discrimination of chlorophenol isomers using mass-selected ion kinetic energy (MIKE) spectrometry [39] and resonant dissociative electron attachment (DEA) have been reported [40,41]. The MIKE spectra result from dissociation of metastable positive ions [42,43], whereas DEA results from dissociation of negative ions [44–46]. MIKE spectrometry is an MS/MS method, whereas DEA is not. The isomeric differentiation observed for the MIKE spectra was explained by a 'ring-walk' mechanism for the chlorine (Cl) atom via a chlorine-bridged state to explain the loss of hydrogen chloride (HCl) [39]. The 'ring-walk' mechanism has also been used to explain the loss of hydrogen fluoride (HF) or difluorocarbene (CF_2) from protonated polyfluorobenzenes [47–51]. The loss of carbon monoxide (CO) from the chlorophenol ions has also been reported by several authors [52–56].

The dissociation of ions can be studied easily using mass spectrometry because the ions can be analyzed and detected, but information about unstable neutral species is limited because analysis of neutral species is difficult due to their lack of electronic charge. Information about the dissociation mechanism of excited neutral species is vital for understanding the important role they play as intermediates in many chemical reactions, and the study of dissociation of these neutral intermediates can provide fundamental knowledge about these chemical reactions. In the present work, the mechanistic features of the dissociation of neutral species in charge inversion spectrometry are compared with those for MIKE spectrometry, CAD spectrometry, and DEA of chlorophenol isomers, using deuterium-labeled compounds.

2. Experimental

The MS/MS instrument used in this work comprises a Hitachi M80B double focusing mass spectrometer as MS-I to mass-select precursor ions, a 3.7 cm long target chamber, and a toroidal electrostatic analyzer (ESA) which is the same type as that in the Hitachi M80B, as MS-II to mass-analyze secondary ions [27,31]. Positive precursor ions are formed by electron ionization (EI) and accelerated to a kinetic energy of 3.0 keV. The precursor ions are mass-selected by MS-I and collide with the alkali metal target in the target chamber. The alkali metal target is introduced into the chamber as a vapor from a reservoir through a ball valve. The target chamber, the ball valve and the reservoir are thermally controlled in order to control the alkali metal density in the target chamber. The detector is a 10 kV post-acceleration secondary electron multiplier, which can detect both positive and negative ions upon application of a suitable polarity.

CAD spectra were measured by mass analyzing the positive ions exiting the target chamber by scanning the ESA voltage, as for a usual CAD measurement. By changing the polarity of MS-II and multiplier, charge inversion spectra were measured by mass analyzing the negative ions exiting from the target chamber. As it takes less than 1 min to change the polarity, charge inversion spectra can be measured using the same conditions for primary ions and target as the CAD spectra, and reproducible CAD and charge inversion can be obtained in a measurement time of a few minutes. An example of a series of such measurements conducted by simply changing the polarity for the measuring the secondary ions is shown in Fig. 1. The similarity of the CAD spectra shown in

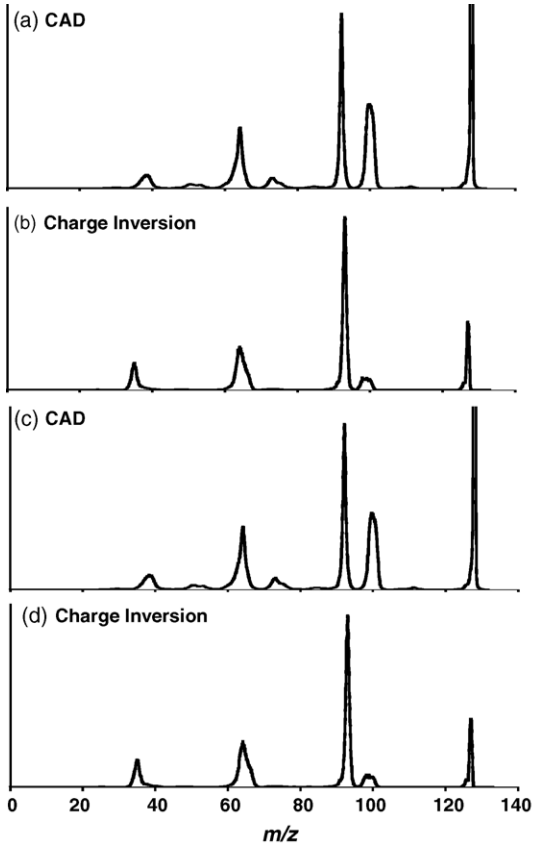

Fig. 1. Collisionally activated dissociation (CAD) spectra, and a charge inversion mass spectrum, measured in series. It takes only a few minutes to measure the respective spectra.

Fig. 1(a) and (c) confirms that these spectra were measured for the same conditions of precursor ions and target density. The conditions for the charge inversion spectrum Fig. 1(b) must, therefore, be the same as those for the CAD spectra, because the charge inversion spectrum was measured between the two CAD spectra measured in this series.

The samples (*o*-, *m*-, and *p*-ClC_6H_4OH, $M_W = 128$), obtained from Tokyo Kasei Co. Ltd., were reagent grade and were used without further purification. The deuterium-labeled isotopomers (*o*-, *m*-, and *p*-ClC_6H_4OD, $M_W = 129$), in which the hydroxyl hydrogen is substituted with deuterium, were obtained by repeated exchange of *o*-, *m*-, and *p*-chlorophenols with D_2O. The degree of labeling, estimated from the peak heights at the mass-to-charge ratio of the appropriate molecular ions, was better than 89%.

3. Results and discussion

3.1. Collisionally activated dissociation spectra

The CAD spectra in Fig. 2 are those of the isomeric chlorophenol ions, $ClC_6H_4OH^+$, and of the partially deuterated forms, $ClC_6H_4OD^+$, obtained using a K target. The $^{35}ClC_6H_4OH^+$ ions of $m/z = 128$ and the $^{35}ClC_6H_4OD^+$ ions of $m/z = 129$, which give rise to the strongest peaks of the molecular ion in the electron ionization spectra, were selected as precursor ions for the spectra shown in Fig. 2(a)–(c) spectra and in Fig. 2(d)–(f), respectively. The peaks at $m/z = 128$ and $m/z = 129$ associated with non-dissociated ions are by far the strongest in the spectra in Fig. 2(a)–(c) and in the spectra in Fig. 2(d)–(f), respectively, as expected. The ordinate values of the spectra in Fig. 2(a)–(c) of the $ClC_6H_4OH^+$ ions are normalized for the peak intensities at $m/z = 100$ in order to assist comparison of the relative peak intensities associated with the various dissociated ions. The peak at $m/z = 92$ is the strongest, and the peaks at $m/z = 64$ and 100 are prominent for the unlabeled *o*-precursor ions, as shown in Fig. 2(a). In the CAD spectra for *m*- and *p*-precursor ions, the peaks at $m/z = 100$ are the strongest, with the peaks at $m/z = 65$ and 92 also being prominent, as shown in Fig. 2(b) and (c), respectively.

The ordinate values of the spectra for the D-labeled chlorophenol isomers in Fig. 2(d)–(f) have been normalized for the peak intensities at $m/z = 101$. The most intense peak in the CAD spectrum of *o*-$^{35}ClC_6H_4OD^+$ ions shown in Fig. 2(d) is that at $m/z = 92$, with the peaks at $m/z = 64$ and 101 also being prominent. For *m- and p*-precursor ions of the D-labeled isomers, the most prominent peaks are those at $m/z = 101$, 92 and 66, as shown in Fig. 2(e) and (f), respectively. From the shifts in the m/z values for the peaks of the D-labeled compounds compared with the unlabeled compounds, the peaks at $m/z = 92$ and 100 for all unlabeled isomers can be assigned unambiguously to $C_6H_4O^+$

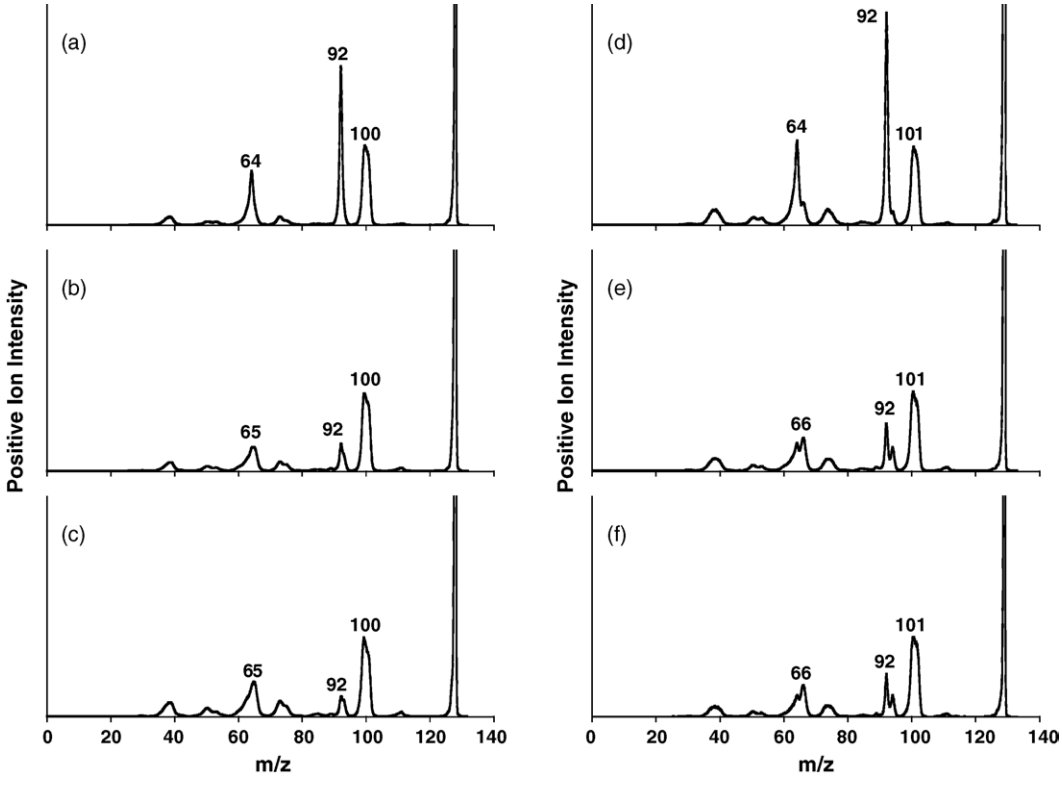

Fig. 2. CAD spectra of $ClC_6H_4OH^+$ ions of *o*-, *m*-, and *p*-chlorophenol, denoted by (a), (b), and (c), respectively and those of partially deuterated $ClC_6H_4OD^+$ ions of *o*-, *m*-, and *p*-chlorophenol, denoted by (d), (e), and (f), respectively. The accelerated energy is 3.0 keV and the target is K. The ordinate of each spectrum has been normalized for the peak intensities at $m/z = 100$ for (a)–(c), and at $m/z = 101$ for (d)–(f).

ions resulting from loss of HCl fragments containing the hydroxyl hydrogen, and $C_5H_5Cl^+$ ions resulting from loss of CO fragments, respectively. From the relative intensities of the peaks at $m/z = 64$ and 92 in both unlabeled and labeled *o*-chlorophenol precursors, the peaks at $m/z = 64$ are assigned to $C_5H_4^+$ ions resulting from combined loss of HCl fragments containing the hydroxyl hydrogen, and CO fragments.

Regarding HCl loss from chlorophenol ions, it has been found from MIKE spectra of unlabeled and labeled chlorophenols [39] that the hydroxyl hydrogen is eliminated by combining with the Cl atom in the *o*-position, and the order of the relative abundances of the ions resulting from loss of HCl compared with those arising from CO loss was found to be *ortho* > *meta* > *para* [39]. From the isomeric dependence of the relative abundances in the MIKE spectra, the loss of HCl from *m*- and *p*-isomers was explained using the 'ring-walk' mechanism. From the CAD spectra of the *m*- and *p*-isomers shown in Fig. 2(b) and (c), it can be seen that the dependency of the intensities of the peaks associated with HCl loss relative to those associated with CO loss for these two isomers is smaller than in the MIKE spectra. The weaker isomeric dependence of the relative extents of loss of HCl and CO observed in this work is attributed to the higher internal energy of the precursor ions [29,31,57] and the shorter available time for dissociation by 'ring-walk' of the Cl atom on the benzene ring in CAD spectrometry compared with MIKE spectrometry.

The loss of CO from chlorophenol cations is also well established [52–56]. Loss of CO from the molecular cation necessarily includes transfer of the hydrogen atom on the hydroxyl group into the benzene ring and, after CO loss, formation of a five-member ring structure has been inferred [52]. While the peak at $m/z = 100$ resulting from CO loss from the chlorophenol isomeric ions is small in electron ionization spectra, it is a major peak in MIKE spectra.

The two-step consecutive loss of CO with Cl loss or HCl loss results in a $C_5H_5^+$ ion ($m/z = 65$) or a $C_5H_4^+$ ion ($m/z = 64$), respectively [53–56]. While the molecular ions with higher internal energy formed by electron ionization produce the $C_5H_5^+$ ion or the $C_5H_4^+$ ion after the consecutive loss of CO and Cl or HCl, those with lower internal energy provide intense $C_5H_5Cl^+$ ions due to loss of CO only, as shown in the MIKE spectra and the CAD spectra. Since the loss of CO involves the re-arrangement of the hydroxyl hydrogen, the prominent peaks in the CAD spectra associated with HCl loss or CO loss are confirmed to represent ions formed via re-arrangement of the hydroxyl hydrogen.

The small peaks at $m/z = 94$ in the CAD spectra of the *m*- and *p*-isomers of the D-labeled precursor (Fig. 2(e) and (f)), and the shoulders at $m/z = 93$ observed in the spectra of the unlabeled precursors, confirm that the loss of Cl atoms from the precursor ions also occurs to some extent. The small peaks at $m/z = 66$ observed in the CAD spectra of the *m*- and *p*-isomers of the labeled precursor are assumed to be associated with $C_5H_4D^+$ ions resulting from consecutive loss of CO and Cl [53–56]. Apart from the peaks at $m/z = 64$ and 92 associated with loss of both CO and HCl, and loss of HCl only, respectively, the CAD spectra show almost no isomeric dependence. A clear difference in the relative intensities of the peaks at $m/z = 64$ and 92 is observed for both the unlabeled and labeled *o*-isomers of chlorophenol compared with the other two isomers. This isomeric differentiation is attributed to the necessary re-arrangement of the hydroxyl hydrogen atom in the major dissociation processes of chlorophenol cations in CAD and MIKE spectrometry, and the time required for this re-arrangement to occur according to the 'ring walk' mechanism.

3.2. Charge inversion spectra

Fig. 3 shows the charge inversion spectra of $ClC_6H_4OH^+$ ions of *ortho*-, *meta*-, and *para*-chlorophenols, and those for partially deuterated $ClC_6H_4OD^+$ ions obtained using a Cs target. The $^{35}ClC_6H_4OH^+$ ions at $m/z = 128$ for unlabeled chlorophenols and the $^{35}ClC_6H_4OD^+$ ions at $m/z = 129$ for D-labeled chlorophenols were selected as precursor ions for all spectra in Fig. 3, as was the case for the CAD spectra. The ordinate of these charge inversion spectra were normalized at the strongest peaks in the respective spectra. In the charge inversion spectra shown in Fig. 3, non-dissociative peaks were not observed, in contrast to the CAD spectra shown in Fig. 2. While peaks at $m/z = 35$, 93, and 127 are prominent for all precursor ions of unlabeled compounds, as shown in Fig. 3(a)–(c), peaks at $m/z = 35$, 94, and 127 are prominent for all precursor ions of D-labeled compounds, as shown in Fig. 3(d)–(f).

From the lack of dependence on labeling of the peaks at $m/z = 35$ and 127 for all isomers, these peaks can clearly be assigned to Cl^- ions, and $ClC_6H_4O^-$ ions formed by the loss of the hydroxyl hydrogen, respectively. The peak at $m/z = 93$ for all unlabeled isomers is assigned to $C_6H_4OH^-$ ions resulting from Cl loss, based on the shift of the m/z values that occurs for the D-labeled isomers. Small peaks at $m/z = 64$ and 99 are observed in all spectra, and from the peak broadening observed in the D-labeled compounds, the broad peak at $m/z = 64$ is assumed to be associated with both $C_5H_4^-$ ions ($m/z = 64$), and $C_5H_5^-$ ions ($m/z = 65$) that contain the hydroxyl hydrogen. Since the peak shape and peak position of the broad peaks at $m/z = 99$ are independent of D-labeling, the peaks at $m/z = 99$ are assumed to be associated with $C_5H_4Cl^-$ ions resulting from loss of COH including the hydroxyl hydrogen.

Small shoulders at $m/z = 92$ are observed in all isomeric spectra of both unlabeled and D-labeled compounds. The m/z values of 35, 93, and 127 for the dominant peaks in the charge inversion spectra are clearly different from those of 64, 65, 92, and 100 in the CAD spectra. The Cl^- ions ($m/z = 35$) and the $ClC_6H_4O^-$ ions ($m/z = 127$) are formed by simple bond cleavages. The one mass unit difference in the intense peak at $m/z = 93$ in the charge inversion spectra and that at $m/z = 92$ in the CAD spectra clearly indicates that the dissociation process in the charge inversion spectrometer is simple cleavage

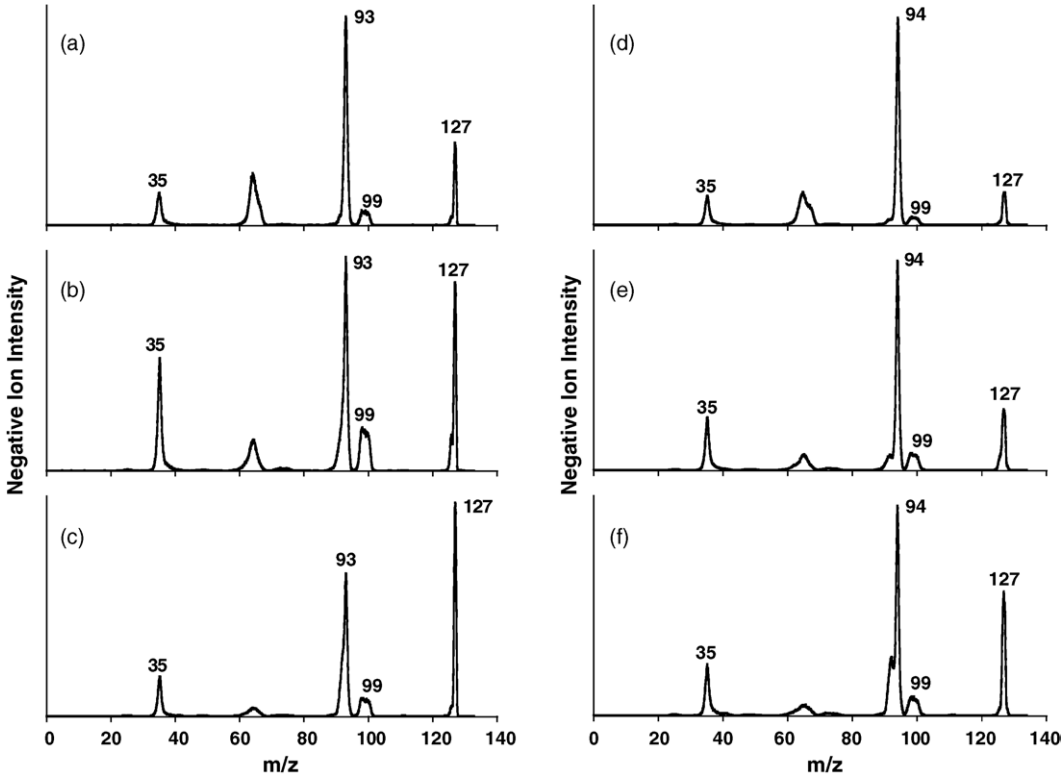

Fig. 3. Charge inversion spectra of $ClC_6H_4OH^+$ ions of *o*-, *m*-, and *p*-chlorophenol, denoted by (a), (b), and (c), respectively and those of partially deuterated $ClC_6H_4OD^+$ ions of *o*-, *m*-, and *p*-chlorophenol, denoted by (d), (e), and (f), respectively. The accelerated energy is 3.0 keV and the target is Cs.

of the Cl fragment without re-arrangement of the hydroxyl hydrogen atom.

The clearest differences in the peak intensities between unlabeled and D-labeled compounds, for all isomeric precursors, are found in the relative intensities of the peaks associated with $C_6H_4OH^-$ ($m/z = 93$ or 94) resulting from Cl loss, relative to the peaks at $m/z = 127$ corresponding to $ClC_6H_4O^-$ formed by loss of the hydroxyl hydrogen. The zero-point vibrational energy of OH is about 1.4 times larger than that of OD [58], resulting in the bond dissociation energy of OH being smaller than that of OD. Consequently, the intensity of the peaks associated with $ClC_6H_4O^-$ ions resulting from OH bond dissociation in the unlabeled compound is expected to be larger than that from OD bond dissociation in the D-labeled compound. Therefore, the observed difference in the intensities of the $ClC_6H_4O^-$ peaks relative to the $C_6H_4OH^-$ peaks for the unlabeled and D-labeled isomers is attributed to a first first-order isotope effect due to this difference in zero-point vibrational energy.

The cross-sections of the fragment negative ions formed from dissociative electron detachment (DEA) for *o*-, *m*-, and *p*-chlorophenols were reported in an electron energy interval of 0–15 eV [40,41]. Dissociation in DEA takes place in the excited negative ions formed by resonant electron attachment. Using the reported values for the cross-sections [40,41], the relative intensities of the negative ions with $m/z = 35$, 93, and 127 are estimated to be approximately 2000, 1, and 40 for *o*-chlorophenol, 1400, 1, 170 for *m*-chlorophenol, and 70, 1, and 200 for *p*-chlorophenol, where the intensity of the peak at $m/z = 93$ in the respective isomers is normalized to unity. The peaks corresponding to the Cl^- ions and the $ClC_6H_4O^-$ ions are much more intense than those for the $C_6H_4OH^-$ ions, for all isomers in DEA. In contrast to these trends in peak intensities, in all of the charge inversion spectra reported in this work, except Fig. 3(c), the $m/z = 93$ peaks for unlabeled compound or the $m/z = 94$ peaks for D-labeled compound are the largest. The large differences between the expected relative peak intensities based on DEA and the measured charge inversion spectra indicate that, unlike the dissociation of negative ions that occurs in DEA, the dissociation in the charge inversion process occurs in the neutral species formed on near-resonant electron transfer to positive ions. Furthermore, the dominant processes in the dissociation of chlorophenol neutrals in the charge inversion spectrometer were found to be simple cleavage of the hydroxyl bond and the C–Cl bond.

Isomeric differentiation was clearly observed in the intensity of peaks associated with the $C_6H_4OH^-$ ion ($m/z = 93$) relative to those for the $ClC_6H_4O^-$ ion ($m/z = 127$), which are the most intense peaks shown in Fig. 3. The abundance ratios ($m/z = 93$)/($m/z = 127$) in the charge inversion spectra are in the order of *ortho-* > *meta-* > *para-*. In charge inversion mass spectrometry, the relative ion intensities in the spectra depend on both the abundance of the neutral fragments and the cross-section for negative ion formation. The abundances

of neutral fragments are determined by branching ratios in the dissociation processes of the excited neutrals formed from the near-resonant neutralization, whereas the branching ratios are influenced by bond dissociation energies and internal energies.

The abundance ratios ($m/z = 35$)/($m/z = 93$) are in the order *meta-* > *para-* ≈ *ortho-*. Since Cl and C_6H_4OH are complementary fragments from ClC_6H_4OH, the Cl and C_6H_4OH fragments are assumed to have equal abundance for each of the isomeric precursors. Since the cross-section for negative ion formation for Cl ($m/z = 35$) is independent of isomeric precursor, the cross-sections for negative ion formation for C_6H_4OH must depend on the isomeric structure of the C_6H_4OH fragments.

The abundance ratios ($m/z = 35$)/($m/z = 127$) are in the order *meta-* ≈ *ortho-* > *para-*. Since the Cl and ClC_6H_4O fragments result from different dissociation processes, the isomeric difference in this ratio can be explained by a difference in dissociation mechanism. It is possible that the dissociation energies of both C–Cl and O–H bonds might depend on isomeric structure. Although these bond energies have been determined experimentally [40], there is some uncertainty in the reliability of the isomeric differences of the bond energies because these energies were not measured directly but were calculated using thermochemical values. The bond energies determined by ab initio calculation in the B3LYP/aug-cc-pVDZ level [59] are shown in Table 1. The energies of the C–Cl bonds of the chlorophenol isomers are between 3.86 and 3.92 eV, which are higher than those of the O–H bonds which are between 3.50 and 3.62 eV. The order of the C–Cl bond energies is *ortho-* > *para-* > *meta-*, while the order of the O–H bond energies is *ortho-* > *meta-* > *para-*. The weaker C–Cl bond for the *meta*-isomer would be expected to result in more abundant Cl fragments, which would explain the higher ($m/z = 35$)/($m/z = 127$) abundance ratio observed for this isomer compared with the *para*-isomer. Likewise, the order of O–H bond energies shown in Table 1 may explain the larger ($m/z = 35$)/($m/z = 127$) abundance ratios for the *ortho*-isomer compared with the *para*-isomer, as the lower energy of the O–H bond would be expected to provide abundant ClC_6H_4O fragments.

Table 1
C–Cl and O–H bond energies (eV) of chlorophenol isomers evaluated by ab initio calculation of B3LYP/aug-cc-pVDZ level

Bond energy	*ortho-*	*meta-*	*para-*
C–Cl	3.92	3.86	3.89
O–H	3.62	3.58	3.50

However, the variation in both bond energies is less than 0.12 eV for all the isomers, so the order of the ($m/z = 35$)/($m/z = 127$) abundance ratios cannot be explained simply by the difference in bond energies. Since the internal energy of the neutral species formed in the charge inversion mass spectrometer depends on the ionization energy due to

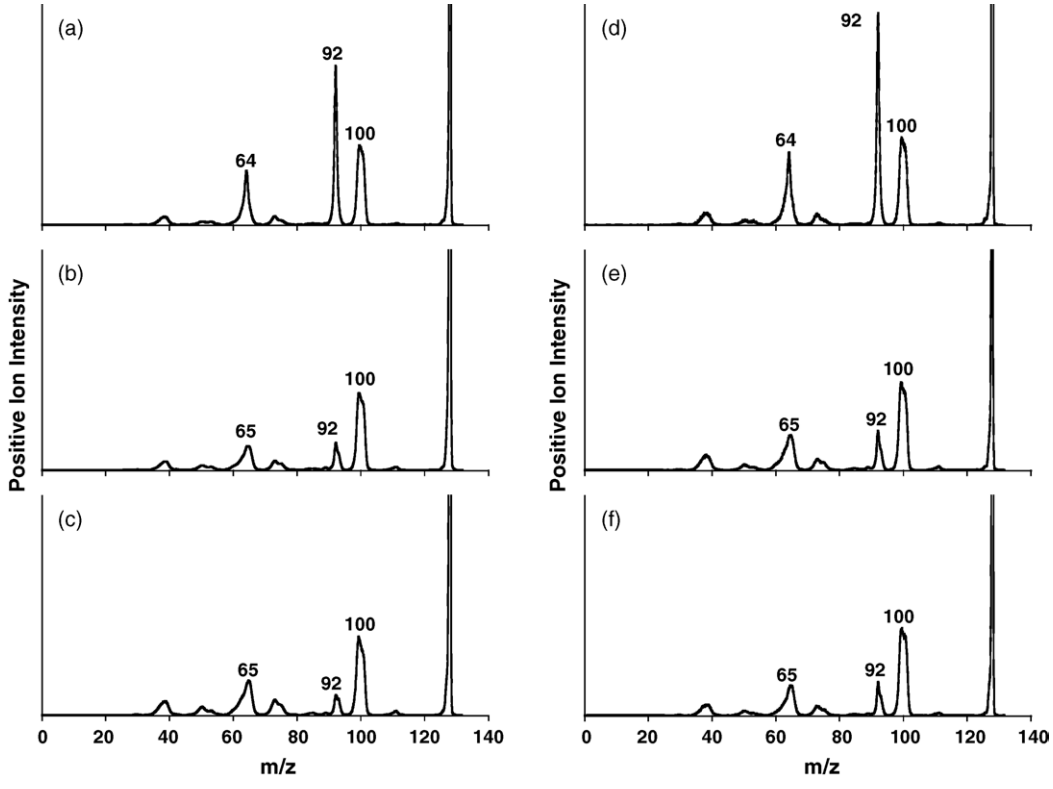

Fig. 4. CAD spectra using K target of *o-*, *m-*, and *p*-chlorophenol, denoted by (a), (b), and (c), respectively, and those using Cs target denoted by (d), (e), and (f), respectively. The ordinate of each spectrum has been normalized for the peak intensities at $m/z = 100$. The spectra (a)–(c) are the same as those shown in Fig. 2(a)–(c).

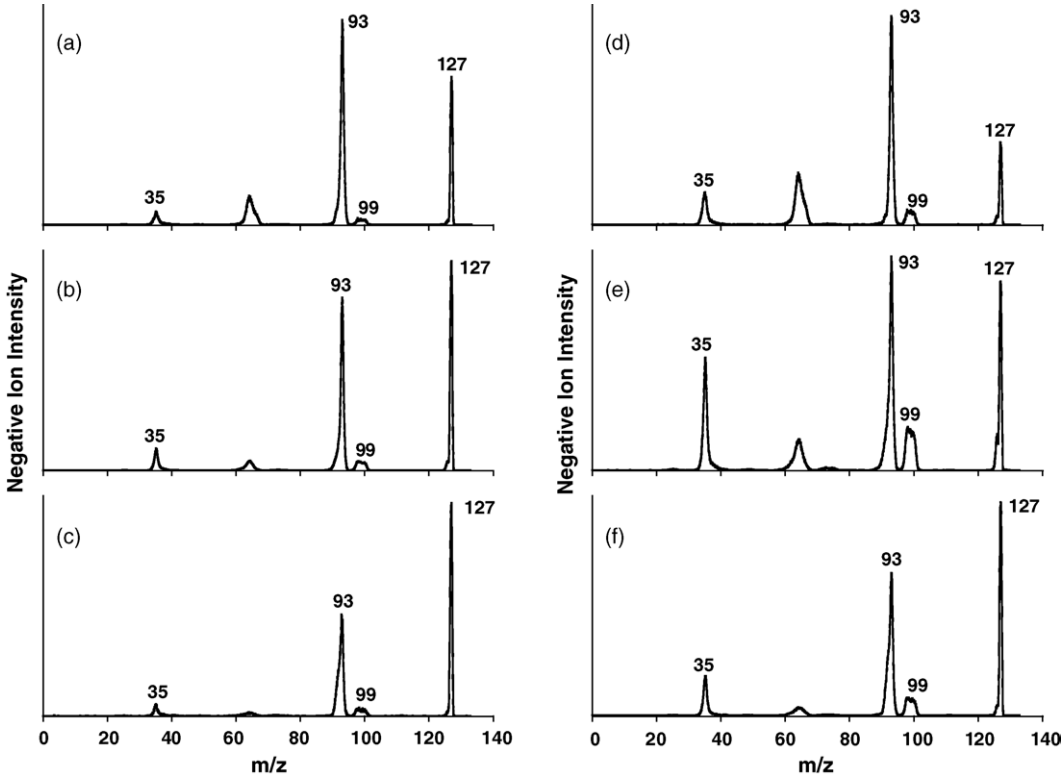

Fig. 5. Charge inversion mass spectra of $ClC_6H_4OH^+$ ions of *o*-, *m*-, and *p*-chlorophenol using K target denoted by (a), (b), and (c), respectively, and those using Cs target denoted by (d), (e), and (f), respectively. The spectra (d)–(f) are the same as those shown in Fig. 3(a)–(c).

the near-resonant neutralization [32], the ionization energy differences could also influence the abundance ratios. As discussed in the case of the ($m/z = 35$)/($m/z = 93$) abundance ratios, the cross-section for $ClC_6H_4O^-$ ion formation may also influence the ($m/z = 35$)/($m/z = 127$) abundance ratios.

3.3. Dependence of spectra on target species

The dependence of the CAD spectra on the target species is shown in Fig. 4. The spectra in Fig. 4(a)–(c) were measured using a K target, and the spectra in Fig. 4(d)–(f) were measured using a Cs target. Only the peak at $m/z = 92$ for the *ortho*-isomer was found to display any appreciable dependence of on the target species, as shown in Fig. 4(a) and (d). The internal energy distribution for collisional activation in the keV energy range is independent of the target species [29,31,57]. The empirical observation that quite different targets often function with similar effectiveness in CAD spectrometry was explained as being due to the same internal energy distribution [60], and examples for $C_6H_4Cl_2^+$, $C_2H_2^+$ and $C_3H_4^+$ isomers have been reported previously [24–28].

The dependence of the charge inversion spectra on the target species are shown in Fig. 5. Since the CAD spectra in Fig. 4 and the charge inversion spectra in Fig. 5 were measured in series for the respective precursors, the experimental conditions used to measure each spectrum in Fig. 5 are the same as those for the spectra in Fig. 4 (see Fig. 1). In contrast to the CAD spectra in Fig. 4, the charge inversion spectra in Fig. 5 display a clear difference between the K and Cs targets for each of the isomeric precursor ions. The intensities of the peaks at $m/z = 35$ and 93 relative to the peak at $m/z = 127$ are obviously larger in the spectra obtained using the Cs target than for the K target for each of the isomeric precursors. Since the neutralization process in charge inversion with an alkali metal target is near resonant, the internal energy of the neutral species formed with a Cs target will be higher than that with a K target [30,31]. Therefore, since the energy of C–Cl bonds is larger than that of O–H bonds, as shown in Table 1, this dependence on the target species is explained by the energy dependence of dissociation in the neutral species.

The intensity of the peak at $m/z = 35$ relative to the peak at $m/z = 93$ is larger with the Cs target than with the K target for the *m*- and *p*-isomers. This difference is attributed to the difference in cross-sections for negative ion formation for Cl and C_6H_4OH, because Cl and C_6H_4OH are complementary fragments of the same precursor. This result demonstrates discrimination among the chlorophenol isomers based on simple bond cleavage is possible using charge inversion spectrometry.

4. Conclusion

In the CAD spectra, the prominent peaks are associated with the $C_6H_4O^+$ and $C_5H_5Cl^+$ ions which form on the dissociation of positive ions resulting in HCl loss and CO loss,

respectively, and these ions were confirmed to be formed via re-arrangement of the hydroxyl hydrogen. The isomeric differentiation observed for these peaks in the CAD and MIKE spectra is related to the time required for re-arrangement according to the 'ring-walk' mechanism. In the charge inversion spectra, the peaks associated with the Cl^-, $C_6H_4OH^-$, and $ClC_6H_4O^-$ ions are dominant. The differences between the dominant peaks in the CAD spectra and those in the charge inversion spectra clearly indicate that the dissociation in the charge inversion spectrometer is via simple bond cleavage without re-arrangement of a hydrogen atom. The large differences in the relative peak intensities between dissociative electron attachment (DEA) and the charge inversion spectra indicate that the dissociation in the charge inversion process takes place in the neutral species formed from near-resonant electron transfer of positive ions, and not dissociation of negative ions as in the case of DEA. The differences in the relative intensities of the dominant peaks among the charge inversion spectra, the CAD spectra and DEA spectra provides further evidence that the isomeric difference observed in the charge inversion spectra is achieved by the simple bond cleavage from the excited neutrals formed via resonant neutralization, whereas the isomeric differentiation of positive ions in CAD spectra is due to the rate of hydrogen atom transfer in the re-arrangement process. The charge inversion spectra of Fig. 5 clearly demonstrate a difference between K and Cs targets for all the isomeric precursor ions, in contrast to the CAD spectra in Fig. 4. The difference in the charge inversion spectra for the K and Cs targets demonstrates the importance of the selected internal energy for enabling isomeric differentiation.

Acknowledgements

Grant-in-Aid for scientific research from Ministry of Education, Culture, Sports, Science and Technology under Grant No. 13640515 is gratefully acknowledged. We gratefully acknowledge the support of Library and Science Information Center, Osaka Prefecture University.

References

[1] M.P. Esposito, H.M. Drake, J.A. Smith, T.W. Owens, United States Environmental Protection Agency Research Reporting Series (EPA-600/2-80-156), Dioxins: Source, Exposure, Transport, and Control, vol. I, National Technical Information Service, Springfield, 1980.
[2] A. Poland, E. Glover, A.S. Kende, J. Biol. Chem. 251 (1976) 4936.
[3] E.E. McConnell, J.A. Moore, Toxicol. Appl. Pharmacol. 37 (1976) 146.
[4] G. Choudhary, L.H. Keith, C. Rappe (Eds.), Chlorinated Dioxins and Dibenzofurans in the Total Environment, Butterworth, Boston, 1983.
[5] S. Safe, O. Hutzonger, T.A. Hill (Eds.), Polychlorinated Dibenzo-*p*-dioxins and -Furans (PCDDs/PCDFs): Sources and Environmental Impact, Epidemiology, Mechanisms of Action, Health Risks, Springer-Verlag, Berlin, 1990.
[6] A. Schecter (Ed.), Dioxins and Health, Plenum, New York, 1994.
[7] J.P. Crine (Ed.), Hazards, Decontamination, and Replacement of PCB: A Comprehensive Guide, Plenum, New York, 1988.
[8] J. Mes, Bull. Environ. Contam. Toxicol. 48 (1992) 815.
[9] R.H. Hill Jr., D.L. Ashley, S.L. Head, L.L. Needham, J.L. Pirkle, Arch. Environ. Health 50 (1995) 277.
[10] C.J.H. Miermans, L.E. van der Velde, P.C.M. Frintrop, Chemosphere 40 (2000) 39.
[11] United States Environmental Protection Agency (EPA 821-B-94-005), Method 1613 Revision B: Tetra- through Octa-Chlorinated Dioxines and furans by Isotope Dilution HRGC/HRMS, EPA, Washington, 1994.
[12] H.R. Buser, Anal. Chem. 48 (1976) 1553.
[13] H.R. Buser, H.P. Bosshardt, C. Rappe, Chemospere 7 (1978) 165.
[14] H.R. Buser, Chemospere 8 (1979) 251.
[15] H.R. Buser, C. Rappe, Anal. Chem. 52 (1980) 2257.
[16] H.R. Buser, C. Rappe, Anal. Chem. 56 (1984) 442.
[17] V.Y. Taguchi, E.J. Reiner, D.T. Wang, O. Meresz, B. Hallas, Anal. Chem. 60 (1988) 1429.
[18] K.L. Busch, G.L. Glish, S.A. McLuckey, Mass Spectrometry/Mass Spectrometry: Technique and Application of Tandem Mass Spectrometry, VCH, New York, 1988 (Chapter 6.1).
[19] D.J. Harvan, J.R. Hass, J.L. Schroeder, B.J. Corbett, Anal. Chem. 53 (1981) 1755.
[20] R.D. Voyksner, J.R. Hass, G.W. Sovocool, M.M. Bursey, Anal. Chem. 55 (1983) 744.
[21] B. Shushan, J.E. Fulford, B.A. Thomson, W.R. Davidson, L.M. Danylewych, A. Ngo, S. Nacson, S.D. Tanner, Int. J. Mass Spectrom. Ion Phys. 46 (1983) 225.
[22] J.B. Plomley, R.E. March, R.S. Mercer, Anal. Chem. 68 (1996) 2345.
[23] R.E. March, M. Splendore, E.J. Reiner, R.S. Mercer, J.B. Plomely, D.S. Waddell, K.A. MacPherson, Int. J. Mass Spectrom. 197 (2000) 283.
[24] S. Hayakawa, K. Taguchi, R. Kotani, K. Arakawa, N. Morishita, J. Mass Spectrom. Soc. Jpn. 49 (2001) 219.
[25] S. Hayakawa, M. Takahashi, K. Arakawa, N. Morishita, J. Chem. Phys. 110 (1999) 2745.
[26] S. Hayakawa, K. Tomozawa, T. Takeuchi, K. Arakawa, N. Morishita, Chem. Phys. Phys. Chem. 5 (2003) 2386.
[27] S. Hayakawa, H. Endoh, K. Arakawa, N. Morishita, T. Sugiura, Int. J. Mass Spectrom. Ion Proc. 151 (1995) 89.
[28] S. Hayakawa, H. Endoh, K. Arakawa, N. Morishita, Int. J. Mass Spectrom. Ion Proc. 171 (1997) 204.
[29] S. Hayakawa, K. Harada, K. Arakawa, N. Morishita, J. Chem. Phys. 112 (2000) 8432.
[30] S. Hayakawa, K. Harada, N. Watanabe, K. Arakawa, N. Morishita, Int. J. Mass Spectrom. 202 (2000) A1.
[31] S. Hayakawa, Int. J. Mass Spectrom. 212 (2001) 229.
[32] S. Hayakawa, J. Mass Spectrom. 39 (2004) 111.
[33] R. Feng, C. Wesdemiotis, M.Y. Zhang, M. Marchetti, F.W. McLafferty, J. Am. Chem. Soc. 111 (1989) 1986.
[34] M.Y. Zhang, C. Wesdemiotis, M. Marchetti, P.O. Danis, J.C. Ray Jr., B.K. Carpenter, F.W. McLafferty, J. Am. Chem. Soc. 111 (1989) 8341.
[35] F.W. McLafferty, C. Wesdemiotis, Org. Mass Spectrom. 24 (1989) 663.
[36] D.E. Drinkwater, A. Fura, M.Y. Zhang, F.W. McLafferty, Org. Mass Spectrom. 26 (1991) 1032.
[37] F.W. McLafferty, Int. J. Mass Spectrom. Ion Proc. 118/119 (1992) 221.
[38] S.R. Heller, G.W.A. Miline, EPA/NIH Mass Spectral Data Base, vol. 1, NSRDS-NBS 63, U.S. Government, Washington, 1978, p. 128.
[39] Y. Takahashi, T. Higuchi, O. Sekiguchi, M. Ubukata, S. Tajima, Rapid Commun. Mass Spectrom. 13 (1999) 393.
[40] R.V. Khatymov, M.V. Muftakhov, P.V. Schukin, V.A. Mazunov, Russ. Chem. Bull., Int. Ed. 52 (2003) 1974.
[41] R.V. Khatymov, M.V. Muftakhov, V.A. Mazunov, Rapid Commun. Mass Spectrom. 17 (2003) 2327.

[42] R.G. Cooks, J.H. Beynon, R.M. Caprioli, G.R. Lester, Metastable Ions, Elsevier, Amsterdam, 1973.
[43] K.L. Busch, G.L. Glish, S.A. McLuckey, Mass Spectrometry/Mass spectrometry: Technique and Application of Tandem Mass Spectrometry, VCH, New York, 1988 (Chapter 3.2).
[44] V.I. Khvostenko, S.R. Rafikov, Dokl. Phys. Chem. 220 (1975) 107.
[45] M.V. Muftakhov, Y.V. Vasil'ev, R.V. Khatymov, V.A. Mazunov, V.V. Takhistov, O.V. Travkin, E.V. Yakovleva, Rapid Commun. Mass Spectrom. 13 (1999) 912.
[46] Y.V. Vasil'ev, M.V. Muftakhov, G.M. Tuimedov, R.V. Khatymov, R.R. Abzalimov, V.A. Mazunov, V.V. Takhistov, T. Drewello, Int. J. Mass Spectrom. 205 (2001) 119.
[47] F. Cacase, M. Speranza, J. Am. Chem. Soc. 98 (1976) 7305.
[48] J. Hrušák, Org. Mass Spectrom. 25 (1990) 503.
[49] M. Tkaczyk, A.G. Harrison, Int. J. Mass Spectrom. 100 (1990) 133.
[50] J. Hrušák, D. Schröder, T. Weiske, H. Schwarz, J. Am. Chem. Soc. 115 (1993) 2015.
[51] S. Tajima, M. Ueki, S. Tajima, O. Sekiguchi, A. Shigihara, Rapid Commun. Mass Spectrom. 10 (1996) 1076.
[52] T.L. Folk, L.G. Wideman, J. Chem. Soc., Chem. Commun. (1969) 491.
[53] M.J. Lacey, C.G. MacDonald, Int. J. Mass Spectrom. Ion Phys. 30 (1979) 359.
[54] C.J. Porter, C.J. Proctor, J.H. Beynon, Org. Mass Spectrom. 16 (1981) 62.
[55] B. Shushan, R.K. Boyd, Int. J. Mass Spectrom. Ion Phys. 37 (1981) 369.
[56] S. Tamburini, P.A. Vigato, P. Traldi, Org. Mass Spectrom. 21 (1986) 183.
[57] V.H. Wysocki, H.I. Kenttämaa, R.G. Cooks, Int. J. Mass Spectrom. Ion Proc. 75 (1987) 181.
[58] R.S. Berry, S.A. Rice, J. Ross, Physical Chemistry, Wiley, New York, 1980, p. 259.
[59] M.J. Frisch, G.W. Trucks, H.B. Schlegel, G.E. Scuseria, M.A. Robb, J.R. Cheeseman, J.A. Montgomery, Jr., T. Vreven, K.N. Kudin, J.C. Burant, J.M. Millam, S.S. Iyengar, J. Tomasi, V. Barone, B. Mennucci, M. Cossi, G. Scalmani, N. Rega, G.A. Petersson, H. Nakatsuji, M. Hada, M. Ehara, K. Toyota, R. Fukuda, J. Hasegawa, M. Ishida, T. Nakajima, Y. Honda, O. Kitao, H. Nakai, M. Klene, X. Li, J.E. Knox, H.P. Hratchian, J.B. Cross, C. Adamo, J. Jaramillo, R. Gomperts, R.E. Stratmann, O. Yazyev, A.J. Austin, R. Cammi, C. Pomelli, J.W. Ochterski, P.Y. Ayala, K. Morokuma, G.A. Voth, P. Salvador, J.J. Dannenberg, V.G. Zakrzewski, S. Dapprich, A.D. Daniels, M.C. Strain, O. Farkas, D.K. Malick, A.D. Rabuck, K. Raghavachari, J.B. Foresman, J.V. Ortiz, Q. Cui, A.G. Baboul, S. Clifford, J. Cioslowski, B.B. Stefanov, G. Liu, A. Liashenko, P. Piskorz, I. Komaromi, R.L. Martin, D.J. Fox, T. Keith, M.A. Al-Laham, C.Y. Peng, A. Nanayakkara, M. Challacombe, P.M.W. Gill, B. Johnson, W. Chen, M.W. Wong, C. Gonzalez, J.A. Pople, Gaussian 03, Revision B.05, Gaussian, Inc., Pittsburgh PA, 2003.
[60] R.G. Cooks, in: R.G. Cooks (Ed.), Collision Spectroscopy, Plenum, New York, 1978, p. 357.